

# The Electromagnetic Field Stress Tensor between Dielectric Half-Spaces

V. Sopova\* and L. H. Ford†

*Institute of Cosmology*

*Department of Physics and Astronomy*

*Tufts University, Medford,*

*Massachusetts 02155*

## Abstract

The stress tensor for the quantized electromagnetic field is calculated in the region between a pair of dispersive, dielectric half-spaces. This generalizes the stress tensor for the Casimir energy to the case where the boundaries have finite reflectivity. We also include the effects of finite temperature. This allows us to discuss the circumstances under which the weak energy condition and the null energy condition can be violated in the presence of finite reflectivity and finite temperature.

PACS numbers: 12.20.Ds, 04.62.+v, 03.70.+k, 77.22.Ch

---

\*Electronic address: [vasilka.sopova@tufts.edu](mailto:vasilka.sopova@tufts.edu)

†Electronic address: [ford@cosmos.phy.tufts.edu](mailto:ford@cosmos.phy.tufts.edu)

## I. INTRODUCTION

The Casimir force [1] between a pair of parallel, perfectly reflecting plates is remarkable prediction of quantum electrodynamics which has been confirmed by experiment [2–7]. It also has some implications for the semiclassical theory of gravity, as the stress tensor of the Casimir energy violates the weak energy condition. Simply from Casimir’s result for the force per unit area, one can construct the entire stress tensor, using conservation, tracelessness and symmetry arguments [8, 9]. The result is

$$T_{\mu\nu} = \begin{pmatrix} T_{00} & 0 & 0 & 0 \\ 0 & T_{xx} & 0 & 0 \\ 0 & 0 & T_{yy} & 0 \\ 0 & 0 & 0 & T_{zz} \end{pmatrix} = \frac{\pi^2}{720 a^4} \begin{pmatrix} -1 & 0 & 0 & 0 \\ 0 & 1 & 0 & 0 \\ 0 & 0 & 1 & 0 \\ 0 & 0 & 0 & -3 \end{pmatrix} \quad (1)$$

Here the plates are separated by a distance  $a$  in the  $z$ -direction, and units where  $\hbar = c = 1$  are used. Here  $T_{\mu\nu}$  is understood to be a renormalized expectation value of the quantum stress tensor operator.

Because the local energy density is negative, the weak energy condition is violated. In addition, the null energy condition,  $T_{\mu\nu}k^\mu k^\nu \geq 0$  for all null vectors  $k_\mu$  is violated as well, except for the case where  $k_\mu$  is parallel to the plates, in which case  $T_{\mu\nu}k^\mu k^\nu = 0$ . The null energy condition is the condition for gravity to locally focus a bundle of null rays. The average null energy condition,

$$\int d\lambda T_{\mu\nu}k^\mu k^\nu \geq 0, \quad (2)$$

along a complete null geodesic, is more difficult to violate [10]. Null rays which are not parallel to the plates eventually intersect and pass through the plates. The integral in Eq. (2) then gets a contribution from the matter composing the plates. The extent to which quantum fields could violate the average null energy condition is of interest in several aspects of gravity theory. Its violation, for example, is essential to construct traversable wormholes [11].

Some authors [12, 13] have suggested that when the assumption of perfect conductivity is removed, the negative energy density might disappear. However, in a previous paper [14], we calculated the energy density between two half-spaces filled with dispersive material, and showed that the energy density in the center can still be negative. However, the energy density is no longer constant in the region between the interfaces, and diverges positively at the boundaries. This divergence, which arises despite a dispersive dielectric function which approaches one at high frequency, can be attributed to the assumption of a sharp boundary between the dielectric and vacuum regions.

It may come as a surprise that the energy density is finite between perfectly reflecting plates, but diverges near plates of finite reflectivity. However, in the perfectly reflecting case there is a cancellation between two divergent terms. Both the mean squared electric field,  $\langle E^2 \rangle$ , and mean squared magnetic field,  $\langle B^2 \rangle$ , diverge but the energy density is finite. When the plates have finite reflectivity, both  $\langle E^2 \rangle$  and  $\langle B^2 \rangle$  diverge less rapidly than in the perfectly reflecting case, but the cancellation is upset, so that the energy density also diverges near the plates. There are more complicated

geometries where similar cancellation can occur. In the interior of a wedge with perfectly reflecting walls, the energy density diverges near the corner, but is finite if one approaches either wall away from the corner [15]. Again there must be a cancellation which would be upset if the wall had finite reflectivity.

In the present paper, we will extend the results of Ref. [14] to study the pressure components of the stress tensor and the effects of finite temperature. As before, our calculations are based on a formalism developed by Schwinger, DeRaad, and Milton [16]. Lorentz-Heaviside units with  $\hbar = c = 1$  will be used.

## II. THE ELECTROMAGNETIC FIELD BETWEEN DIELECTRIC SLABS-CORRECTIONS AT FINITE TEMPERATURE

We consider the electromagnetic field stress tensor in the vacuum region of width  $a$  between two dielectric half-spaces whose dielectric function is described by the plasma model:

$$0 < z < a : \epsilon(z) = 1, \quad (3)$$

$$z < 0 \text{ and } z > a : \epsilon(z) \equiv \epsilon = 1 - \frac{\omega_p^2}{\omega^2}, \quad (4)$$

where  $\omega_p$  is the plasma frequency. The finite mean squared electric field in the vacuum region, at zero temperature, can be expressed as an integral over imaginary frequency  $\zeta$  [14]

$$\begin{aligned} \langle E^2 \rangle = & \frac{1}{2\pi^2} \int_0^\infty d\zeta \int_0^\infty dk \frac{k}{\kappa} \left\{ \zeta^2 \left( \frac{r^2}{r^2 - e^{2\kappa a}} + \frac{r'^2}{r'^2 - e^{2\kappa a}} \right) + \right. \\ & \left. + \left[ -\zeta^2 \frac{r}{1 - r^2 e^{-2\kappa a}} + (2k^2 + \zeta^2) \frac{r'}{1 - r'^2 e^{-2\kappa a}} \right] e^{-\kappa a} \cosh[\kappa(2z - a)] \right\}, \quad (5) \end{aligned}$$

where the reflection coefficients for S and P polarizations, respectively, are given by

$$r = \frac{\kappa - \kappa_1}{\kappa + \kappa_1} \quad (6)$$

$$r' = \frac{\kappa\epsilon - \kappa_1}{\kappa\epsilon + \kappa_1}. \quad (7)$$

The quantities  $\kappa$  and  $\kappa_1$  are defined as  $\kappa^2 = k^2 + \zeta^2$ , and  $\kappa_1^2 = k^2 + \zeta^2\epsilon$ . The expression for the mean squared magnetic field  $\langle B^2 \rangle$  is obtained from that for  $\langle E^2 \rangle$  by interchanging the coefficients  $r$  and  $r'$ . The energy density in the vacuum region,  $U = T_{00} = (\langle E^2 \rangle + \langle B^2 \rangle)/2$  is then

$$\begin{aligned} U = & \frac{1}{2\pi^2} \int_0^\infty d\zeta \int_0^\infty dk \frac{k}{\kappa} \left\{ \zeta^2 \left( \frac{r^2}{r^2 - e^{2\kappa a}} + \frac{r'^2}{r'^2 - e^{2\kappa a}} \right) + \right. \\ & \left. + k^2 \left( \frac{r}{1 - r^2 e^{-2\kappa a}} + \frac{r'}{1 - r'^2 e^{-2\kappa a}} \right) e^{-\kappa a} \cosh[\kappa(2z - a)] \right\}. \quad (8) \end{aligned}$$

As discussed in [14],  $U$  is position dependent: it has a minimum at the center of the vacuum region and diverges at the interfaces. The overall sign of  $U$  at its minimum depends on the choice of  $a$  and  $\omega_p$ . As the product  $\omega_p a$  grows,  $U$  at the midpoint decreases, becoming negative for  $\omega_p a \approx 100$  (see Figure 2, dash-dot line). It is of interest to examine the effects due to finite temperature upon the energy density and see when its sign can still be negative when the temperature is not zero.

For this purpose, we write Eq. (8) as a Fourier series instead of an integral on  $\zeta$  [16]:

$$U_C = \frac{1}{\pi\beta} \sum'_{n=0} \int_0^\infty dk \frac{k}{\kappa} \left\{ \zeta_n^2 \left( \frac{r^2}{r^2 - e^{2\kappa a}} + \frac{r'^2}{r'^2 - e^{2\kappa a}} \right) + k^2 \left( \frac{r}{1 - r^2 e^{-2\kappa a}} + \frac{r'}{1 - r'^2 e^{-2\kappa a}} \right) e^{-\kappa a} \cosh[\kappa(2z - a)] \right\}, \quad (9)$$

where  $\zeta_n = 2\pi n/\beta$ . The prime on the sum is a reminder to count the  $n = 0$  term with half weight, and  $\beta = 1/kT$ . This expression (which vanishes as  $a \rightarrow \infty$ ) represents the Casimir contribution to the energy density, or the difference between the energy density at finite temperature with the dielectric walls present and not. It does not include the energy density of a thermal bath without the walls present. To get the latter energy density, we can start with the full expression for  $U$ , which includes the empty space vacuum divergent term [14]. At zero temperature, this term can be written as an integral over real frequencies:

$$U_{ES} = -\frac{i}{2\pi^2} \int_0^\infty d\omega \int_0^\infty dk k \frac{\omega^2}{\kappa}, \quad (10)$$

where  $\kappa$  is defined as  $\kappa^2 = k^2 - \omega^2$ . For finite temperatures, this term is modified by inserting a factor  $[1 + 2/(e^{\beta\omega} - 1)]$  to account for the thermal energy. This factor reflects the fact that at zero temperature, each mode has an energy of  $\frac{1}{2}\omega$ ; at finite temperature, there is an additional thermal energy of  $1/(e^{\beta\omega} - 1)$ . After removing the divergent term, the result is the familiar result for the energy density of blackbody radiation:

$$\Delta U_{ES} = \frac{\pi^2}{15\beta^4}. \quad (11)$$

The energy density in the vacuum region at finite temperature is then

$$U(T) = U_C + \Delta U_{ES}. \quad (12)$$

Figure 1 shows two graphs representing energy density at zero and finite temperature corresponding to  $\beta/a = 5$ . As expected, the local energy density increases with temperature, and negative energy density is only possible if the temperature is sufficiently low. On the other hand, the zero temperature results are a good approximation so long as  $\beta \gg a$ . For systems at room temperature, this increase in the energy density is still very small when the separations between the walls are of the order of few micrometers. More generally, one can ignore thermal effects at distances

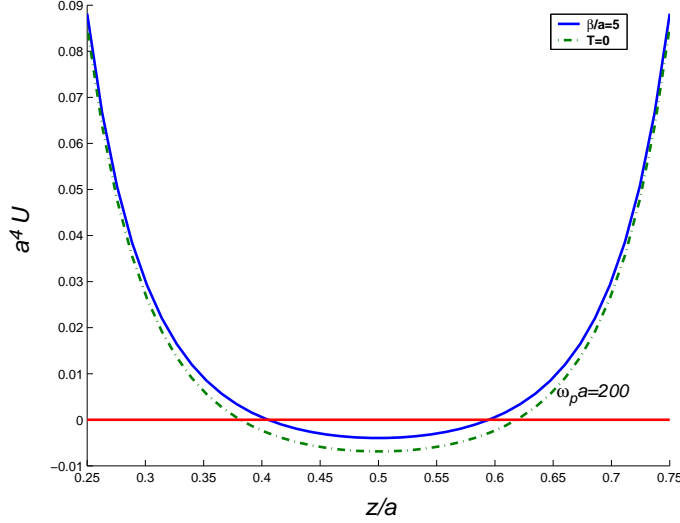


FIG. 1: The solid curve represents the energy density at finite temperature corresponding to  $\beta/a = 5$ , as compared to the energy density at zero temperature (dash-dot line). As expected, the local energy density increases with temperature, and negative energy density is only possible if the temperature is sufficiently low.

small compared to  $1/(kT)$ . In this case, it is still possible to achieve negative energy density in the central region. At room temperature, for example,  $\beta \approx 8 \mu\text{m}$ . Thus,  $\beta/a = 5$  corresponds to  $a = 1.6 \mu\text{m}$ , which is in the range of separations for which Casimir force experiments have been performed.

The energy density at the center of the vacuum region is shown in Fig. 2 as a function of  $\omega_p a$  for various temperatures. As the temperature increases, the region of negative energy density shrinks, and when  $\beta \lesssim 2.6 a$ , the energy density is positive everywhere.

### III. THE TRANSVERSE AND LONGITUDINAL PRESSURE

First consider the longitudinal pressure,  $p_z = T_{zz}$ . The conservation law,  $\partial^\mu T_{\mu\nu} = 0$ , with  $\nu = z$ , and the fact that  $T_{\mu\nu}$  is diagonal, implies that  $\partial^z T_{zz} = 0$ . Thus  $T_{zz}$  is constant. From the relation  $T_{zz} = T_{00} - E_z^2 - B_z^2$ , we find that, at zero temperature,

$$p_z = T_{zz} = \frac{1}{2\pi^2} \int_0^\infty d\zeta \int_0^\infty dk k \kappa \left( \frac{r^2}{r^2 - e^{2\kappa a}} + \frac{r'^2}{r'^2 - e^{2\kappa a}} \right) \quad (13)$$

The plot of this function is shown in Fig. 3 as a function of  $\omega_p a$  at any value of  $z$  in the vacuum region. The horizontal line corresponds to the perfectly reflecting wall,  $p_z = -\pi^2/(240a^4)$ . Note that  $p_z$  is the force per unit area on one half-space due to

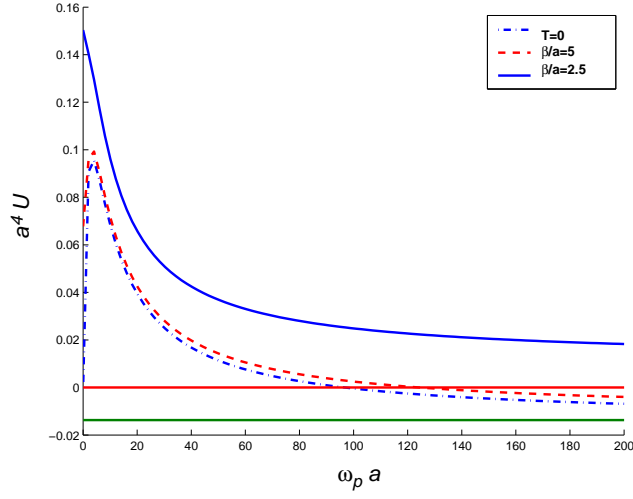


FIG. 2: The figure represents the energy density at the center of the vacuum region as a function of  $\omega_p a$  for various temperatures including zero temperature (dash-dot line). As the temperature grows (and  $\beta$  decreases), the value of  $\omega_p a$  for which the energy density becomes negative shifts towards larger values.

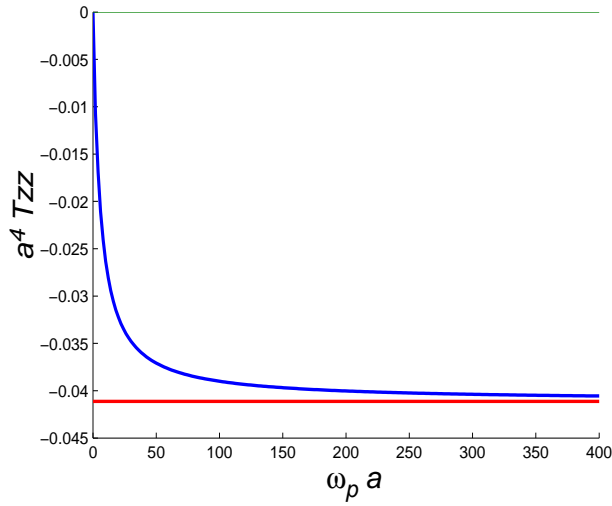


FIG. 3: The graph represents the pressure  $T_{zz}$  as a function of  $\omega_p a$  at zero temperature for all  $0 < z < 1$ . The horizontal line corresponds to the perfectly reflecting wall.

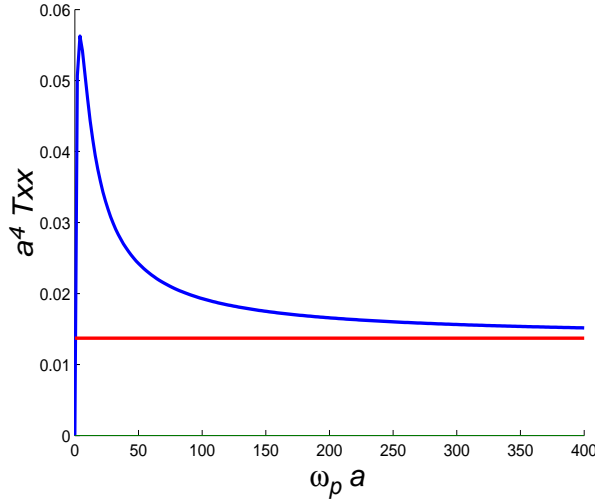


FIG. 4: The graph represents the pressure  $T_{xx}$  at zero temperature as a function of  $\omega_p a$  at  $z = 0.5a$ . The horizontal line corresponds to the perfectly reflecting wall.

the other, and agrees with the result of the Lifshitz theory [16, 17]. The magnitude of the force is maximum in the perfectly conducting limit.

The transverse pressure,  $p_x = T_{xx} = p_y = T_{yy}$  is a nontrivial function of  $z$ , and is given at zero temperature by

$$T_{xx} = -\frac{1}{4\pi^2} \int_0^\infty d\zeta \int_0^\infty dk \frac{k^3}{\kappa} \left\{ \left( \frac{r^2}{r^2 - e^{2\kappa a}} + \frac{r'^2}{r'^2 - e^{2\kappa a}} \right) - \left( \frac{r}{1 - r^2 e^{-2\kappa a}} + \frac{r'}{1 - r'^2 e^{-2\kappa a}} \right) e^{-\kappa a} \cosh[\kappa(2z - a)] \right\}, \quad (14)$$

The plot of this function is shown in Fig. 4 as a function of  $\omega_p a$  at the center of the vacuum region. The horizontal line corresponds to the perfectly reflecting wall.

If we compare the position dependent term in  $U$ , Eq. (8), with that in  $T_{xx}$ , Eq.(14), we see that they differ by a factor of two. These terms are dominant near a wall, so the asymptotic form of  $T_{xx}$  near the boundary  $z = 0$  is one half the corresponding expression for  $U$  in this limit, which was found in Ref. [14]:

$$T_{xx} \sim \frac{1}{2} U \sim \frac{\sqrt{2}\omega_p}{128\pi} \frac{1}{z^3}, \quad \text{as } z \rightarrow 0. \quad (15)$$

Again, this singular behavior arises despite the inclusion of dispersion in our treatment, and can be viewed as due to the assumption of a sharp boundary at  $z = 0$ . A crucial point is that the reflection coefficients vanish as  $\omega^{-2}$  as  $\omega \rightarrow \infty$ . Pfenning [18] has studied scalar models in which these coefficients vanish more rapidly at high frequency, and obtained a finite stress tensor at the boundary.

#### IV. THE NULL ENERGY CONDITION

Now we turn to the null energy condition for rays travelling parallel to the walls. Combining Eqs. (8) ( $T_{00} = U$ ) and (14), and changing variables using  $\zeta = u t$  and  $k = u \sqrt{1 - t^2}$ , we have

$$T_{00} + T_{xx} = \frac{1}{4\pi^2} \int_0^\infty du u^3 \int_0^1 dt \left\{ (3t^2 - 1) \left( \frac{r^2}{r^2 - e^{2ua}} + \frac{r'^2}{r'^2 - e^{2ua}} \right) + 3(1 - t^2) \left[ \frac{r}{1 - r^2 e^{-2ua}} + \frac{r'}{1 - r'^2 e^{-2ua}} \right] e^{-ua} \cosh[u(2z - a)] \right\}. \quad (16)$$

We see that in case of  $r \rightarrow -1$  and  $r' \rightarrow 1$ , or perfectly reflecting walls,  $T_{00} + T_{xx} = 0$ , so the null energy condition is marginally satisfied. We now wish to show that in all other cases,  $T_{00} + T_{xx} > 0$ . First consider the terms proportional to  $3t^2 - 1$ . Of these, the term proportional to  $r^2$  vanishes because  $r$  is independent of  $t$  and  $\int_0^1 dt (3t^2 - 1) = 0$ . Next consider the term proportional to  $3t^2 - 1$  and to  $r'^2$ . Its contribution to the integral on  $t$  can be written, using partial integration, as

$$\int_0^1 dt (3t^2 - 1) \frac{r'^2}{r'^2 - e^{2ua}} = -e^{-2ua} \int_0^1 dt t (1 - t^2) \frac{2r'}{(1 - r'^2 e^{-2ua})^2} \frac{dr'}{dt}, \quad (17)$$

where in terms of the new coordinates,

$$r' = \frac{u^2 t^2 + \omega_p^2 - ut^2 \sqrt{u^2 + \omega_p^2}}{u^2 t^2 + \omega_p^2 + ut^2 \sqrt{u^2 + \omega_p^2}}. \quad (18)$$

Its derivative,

$$dr'/dt = -\frac{4u\omega_p^2 t \sqrt{u^2 + \omega_p^2}}{[ut^2(u + \sqrt{u^2 + \omega_p^2}) + \omega_p^2]^2}, \quad (19)$$

is negative. Thus,

$$\int_0^1 dt (3t^2 - 1) \frac{r'^2}{r'^2 - e^{2ua}} > 0. \quad (20)$$

Now consider the term in Eq. (16) proportional to  $1 - t^2$ . We can write

$$r = \frac{u - \sqrt{u^2 + \omega_p^2}}{u + \sqrt{u^2 + \omega_p^2}}, \quad (21)$$

from which we see that  $r < 0$ . We can also show that

$$r' - |r| = r' + r = \frac{2\omega_p^2(1 - t^2)u}{\sqrt{u^2 + \omega_p^2}(2t^2 u^2 + \omega_p^2) + 2t^2 u^3 + u\omega_p^2(t^2 + 1)} \geq 0, \quad (22)$$



for  $0 \leq t \leq 1$ , from which it follows that  $r' \geq |r| \geq 0$ . This implies that the  $1 - t^2$  term in Eq. (16) is non-negative. Thus  $T_{00} + T_{xx} \geq 0$ , and the null energy condition is satisfied by a finite margin, except for the limiting case of a perfect conductor. This implies that the gravitational effect on light rays moving parallel to the plates is to cause focusing. Even though the energy density can be negative, its effect is more than cancelled by the positive pressure.

Now we inspect the effect of the finite temperature on the null energy condition. We expect that finite temperature would make the null energy condition satisfied by a wider margin. So, we write Eq. (16) as Fourier series as above in Eq. (9):

$$T_{00} + T_{xx} = \frac{1}{2\pi\beta} \sum_{n=0}^{\infty} \int_0^{\infty} dk \frac{k}{\kappa} \left\{ (k^2 - 2\zeta_n^2) \left( \frac{r^2}{e^{2\kappa a} - r^2} + \frac{r'^2}{e^{2\kappa a} - r'^2} \right) - 3k^2 \left( \frac{r}{r^2 e^{-2\kappa a} - 1} + \frac{r'}{r'^2 e^{-2\kappa a} - 1} \right) e^{-\kappa a} \cosh[\kappa(2z - a)] \right\} + \frac{4\pi^2}{45\beta^4}. \quad (23)$$

Evaluated at  $z = 0.5a$ , where it has a minimum, this becomes:

$$(T_{00} + T_{xx})_{z=0.5a} = \frac{1}{2\pi\beta} \sum_{n=0}^{\infty} \int_{\zeta_n}^{\infty} d\kappa \left\{ (\kappa^2 - 3\zeta_n^2) \left( \frac{r^2}{e^{2\kappa a} - r^2} + \frac{r'^2}{e^{2\kappa a} - r'^2} \right) - 3(\kappa^2 - \zeta_n^2) \left( \frac{r}{r^2 e^{-2\kappa a} - 1} + \frac{r'}{r'^2 e^{-2\kappa a} - 1} \right) e^{-\kappa a} \right\} + \frac{4\pi^2}{45\beta^4}. \quad (24)$$

A change of variables  $k \rightarrow \kappa$  has been made. A plot of Eq. (24) as a function of  $\omega_p a$  is shown in Fig. 5. The quantity  $T_{00} + T_{xx}$  is always positive and increases with increasing temperature, so the null energy condition is always satisfied for transverse rays.

Now we examine the null energy condition for light rays perpendicular to the walls. Adding Eqs. (13) and (8) yields, at zero temperature

$$T_{00} + T_{zz} = \frac{1}{2\pi^2} \int_0^{\infty} du u^3 \int_0^1 dt \left\{ (1 + t^2) \left( \frac{r^2}{r^2 - e^{2ua}} + \frac{r'^2}{r'^2 - e^{2ua}} \right) + (1 - t^2) \left[ \frac{r}{1 - r^2 e^{-2ua}} + \frac{r'}{1 - r'^2 e^{-2ua}} \right] e^{-ua} \cosh[u(2z - a)] \right\}. \quad (25)$$

A plot of Eq. (25) as a function of position is shown in Fig. 6 for three values of  $\omega_p a$ . The bottom solid line corresponds to the case of perfectly reflecting walls,  $T_{00} + T_{zz} = -\pi^2/(180a^4)$ , for which the null energy condition in the  $z$  direction is violated. The figure shows that in the case of dielectric walls, the null energy condition can be violated locally in this direction, but only over a restricted interval in the internal region. The average null energy condition integral, Eq. (2), will acquire a net positive contribution even before a null ray reaches a boundary. Finite temperature will further restrict the region where the null energy condition can be violated.

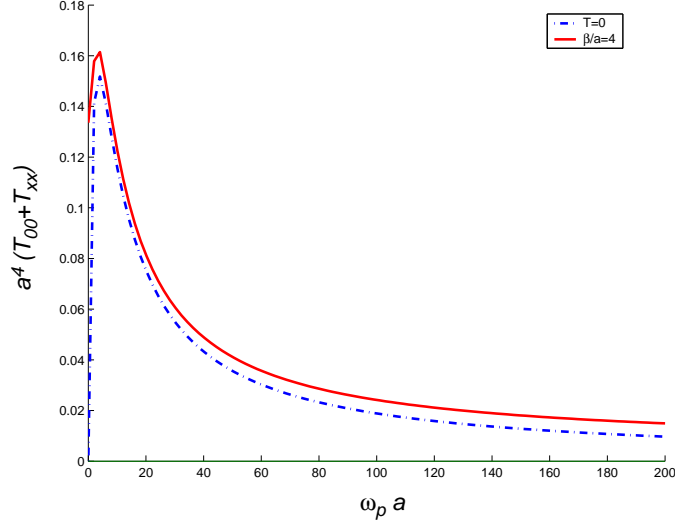


FIG. 5: The solid curve represents the energy density plus pressure as a function of  $\omega_p a$  at  $z = 0.5a$  and at finite temperature corresponding to  $\beta/a = 5$ . The dash-dot line represents the same function at zero temperature. The graph indicates that finite temperature makes the null energy condition in the transverse direction satisfied by a wider margin, as expected.

## V. SUMMARY

In this paper, we have discussed the effects of finite reflectivity of the walls and of finite temperature on the Casimir energy density and pressures. In particular, we have been interested in when the weak energy condition and the null energy condition can be violated. We find that the weak energy condition and the null energy condition for rays not parallel to the plates can still be violated, but with more difficulty than in the case of perfectly reflecting plates. Furthermore, these violations are now confined to a localized central region finitely removed from the boundaries. These regions decrease in size as the temperature increases, and eventually vanish for  $\beta \ll a$ . The energy density and transverse pressure diverge positively as the boundaries are approached, further limiting the region of possible energy condition violation. The null energy condition for rays parallel to the boundary, which is marginally satisfied for the perfectly reflecting case at zero temperature, is satisfied by a finite margin with either finite reflectivity or finite temperature.

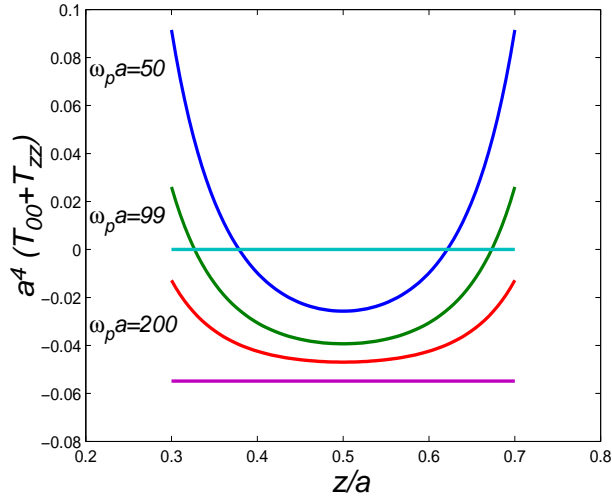


FIG. 6: A plot of  $T_{00} + T_{zz}$  as a function of position is shown for three values of  $\omega_p a$  at zero temperature. The bottom solid line corresponds to the case of perfectly reflecting walls, for which the null energy condition in  $z$  direction is violated. The figure shows that in the case of dielectric walls, the null energy condition can be violated locally in this direction.

### Acknowledgments

This work was partially supported by NSF grant PHY-0244898.

- 
- [1] H.B.G. Casimir, Proc. K. Ned. Akad. Wet. **B51**, 793 (1948).
  - [2] M.Y. Sparnaay, Physica **24**, 751 (1958).
  - [3] S.K. Lamoreaux, Phys. Rev. Lett. **78**, 5 (1997); erratum in Phys. Rev. Lett. **81**, 5475 (1998).
  - [4] U. Mohideen and A. Roy, Phys. Rev. Lett. **81**, 4549 (1998); physics/9805038.
  - [5] A. Roy, C.Y. Lin and U. Mohideen, Phys. Rev. D **60**, 111101(R) (1999); quant-ph/9906062.
  - [6] H.B. Chan, V. A. Aksyuk, R. N. Kleiman, D. J. Bishop and Federico Capasso *et al.*, Science **291**, 1941 (2001).

- [7] G. Bressi, G. Carugno, R. Onofrio and G. Ruoso, Phys. Rev. Lett. **88**, 041804-1 (2002); quant-ph/0203002.
- [8] L. S. Brown and G. J. Maclay, Phys. Rev. **184**, 1272 (1969).
- [9] B.S. DeWitt, Phys. Rep. **19C**, 295 (1975).
- [10] N. Graham, K.D. Olum, and D. Schwartz-Perlov, Phys. Rev. D **70**, 105019 (2004); gr-qc/0407006.
- [11] M. Visser, *Lorentzian Wormholes; From Einstein to Hawking*, (AIP, Woodbury, N. Y., 1995).
- [12] A. D. Helfer and A. S. Lang, J. Phys. A: Math. Gen. **32**, 1937 (1999); hep-th/9810131.
- [13] S. K. Lamoreaux, Am. J. Phys. **67**, 850 (1999).
- [14] V. Sopova and L. H. Ford, Phys. Rev. D **66**, 045026 (2002); quant-ph/0204125.
- [15] V.V. Nesterenko, G. Lambiase and G. Scarpetta, Ann. Phys. (N.Y.) **298**, 403 (2002); hep-th/0202089.
- [16] J. Schwinger, L. L. DeRaad, and K. A. Milton, *Ann. Phys.* (N.Y.) **115**, 1 (1978).
- [17] E.M. Lifshitz, Zh. Eksp. Teor. Fiz. **29**, 94 (1954) [Sov. Phys. JETP **2**, 73 (1956)].
- [18] M.J. Pfenning, Phys. Rev. D **62**, 045018 (2000); hep-th/0001034.